16 Lecture, 26 October 1999

16.1 The van Cittert - Zernike theorem and radio interferometers

The largest single-dish radio telescopes have diffraction-limited resolution no better than tens of arcseconds, but as we have noted, the vast majority of astronomical objects of current interest have most of their important structure on angular scales much smaller than this. Radio-astronomical observations can presently be made with spatial (i.e. angular) resolution below 0.001 arcseconds by use of networks of widely separated telescopes from which signals are combined in a way that allows retrieval of images with angular scales proportional to wavelength divided by the *distance between the telescopes*, rather than the diameter of any individual telescope. The techniques by which these images are obtained are in general called *spatial interferometry* or *aperture synthesis.* This is a very deep subject, worthy of a multi-semester graduate-level course, so we will not attempt to discuss spatial interferometry very thoroughly here. However, our work so far has left us in a good position to understand the basic principles of spatial interferometry, so we will present the following brief introduction.

Imagine an extended source of electromagnetic radiation lying a very great distance r away from a set of observers. It will help to envision the object as a planar section of the celestial sphere, with locations within it described by a Cartesian coordinate system $x'-y'$, as shown in Figure 16.1. If the electric field in this object is given as a function of position on the celestial sphere as $E_N(\boldsymbol{r}',t)$, oscillating with wavelength λ, then a distant observer will measure an electric field given by the Kirchhoff diffraction integral, Equation 12.24:

$$E_F(\boldsymbol{\kappa},t)=\frac{e^{i\kappa r}}{\lambda r}\int E_N(\boldsymbol{r}',t)e^{-i\boldsymbol{\kappa}\cdot\boldsymbol{r}'}da' \quad , \tag{16.1}$$

where the integration bounds are understood in principle to cover the entire sky, even though the source's electric field is assumed to be finite over a small range of angles. Suppose two observers each measure an oscillating electric field due to the nearly planar, slightly spherical wavefronts from the object, one detecting a wavevector $\boldsymbol{\kappa}_1$ and the other $\boldsymbol{\kappa}_2$ with the same magnitude, $2\pi/\lambda$. It turns out to be interesting to consider the *correlation* between their two measurements. Define the *mutual coherence* of the measurements as follows

$$\Gamma(\boldsymbol{\kappa}_1,\boldsymbol{\kappa}_2,0)\equiv\left\langle E_F(\boldsymbol{\kappa}_1,t)E_F^*(\boldsymbol{\kappa}_2,t)\right\rangle=\frac{1}{\tau}\int_0^\tau E_F(\boldsymbol{\kappa}_1,t)E_F^*(\boldsymbol{\kappa}_2,t)dt \quad , \tag{16.2}$$

where the apparently spurious "0" in the argument list for Γ indicates that the measurements refer to the same wavefront; that is, there is zero time delay between the two combined measurements. As can be told from the name, the mutual coherence expresses the degree to which the oscillations detected in the field measurements are *coherent*; if two measurements at different $\boldsymbol{\kappa}$ oscillate at the same frequency and with a constant difference of phase, they are said to be perfectly coherent, and the integral in Equation 16.2 would have a relatively large value. If on the other hand there is no correlation in the oscillations, the integral would have a value approaching zero, and we would say that the corresponding field is *incoherent*. In terms of the properties of the *near* field, the mutual coherence of the far field is obtained simply by inserting Equation 16.1 into 16.2 (twice) and rearranging the integrals a bit:

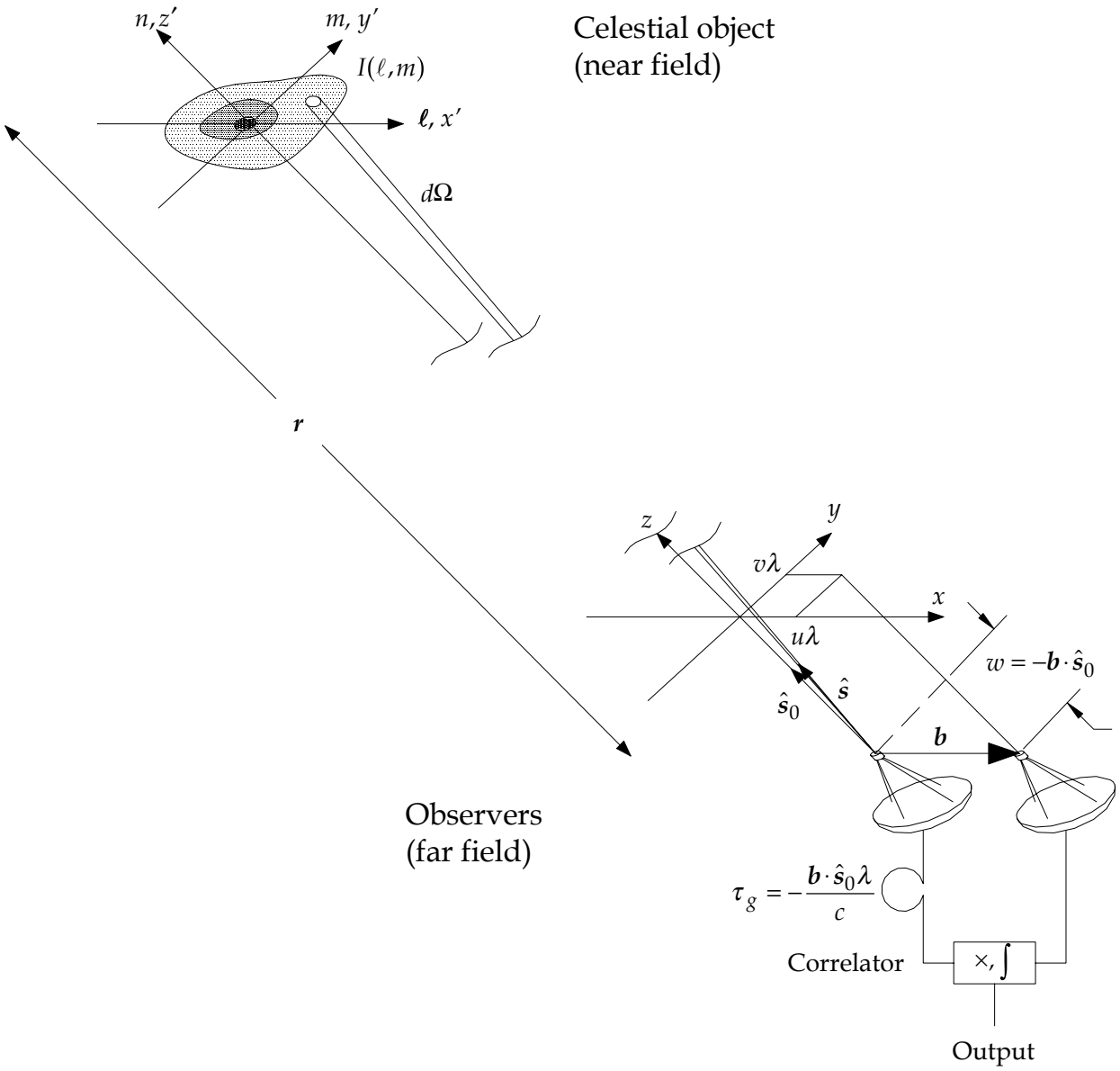

Figure 16.1: geometry of the *u*-*v* plane in which measurements of the mutual coherence of the far field is measured, and the parallel $\ell - m$ plane in which the object's intensity distribution is described. The two-telescope interferometer used to measure the electric fields that go into the mutual coherence, and their aspect with respect to the *u*-*v* and $\ell - m$ planes, are indicated schematically.

$$\Gamma(\boldsymbol{\kappa}_1, \boldsymbol{\kappa}_2, 0) = \frac{e^{i\kappa_1 r_1}}{\lambda r_1} \frac{e^{-i\kappa_2 r_2}}{\lambda r_2} \iint \left(\frac{1}{\tau} \int_0^\tau E_N(\boldsymbol{r}_1', t) E_N^*(\boldsymbol{r}_2', t) dt \right) e^{-i\boldsymbol{\kappa}_1 \cdot \boldsymbol{r}_1'} e^{i\boldsymbol{\kappa}_2 \cdot \boldsymbol{r}_2'} da_1' da_2' \quad . \tag{16.3}$$

Note that since the wavevector magnitudes $\kappa_1 = \kappa_2 = 2\pi / \lambda$, and that $r_1 = r_2 = r$, the exponential factors outside the integrals come to $e^{i\kappa_1 r_1} e^{-i\kappa_2 r_2} = 1$. Also in the integrand is a combination – set off in brackets – that represents the mutual coherence of the near field. Now the near field is that of an astronomical object, and as such we can safely make an important assumption: the near field is *incoherent*. The reason is that

most astronomical objects produce electromagnetic radiation by random, *thermal* processes such as blackbody emission; there is no correlation between the emission per unit time from two different spots within the object, even though their average emission rate may be the same. (Note that incoherence of the near field does not imply incoherence for the far field!) Thus the integral in brackets in Equation 16.3 vanishes unless the two near fields are taken at the same point in the $x'-y'$ plane; it is convenient to write it as a two-dimensional Dirac delta function:

$$\begin{aligned}\frac{1}{\tau}\int_0^\tau E_N(\boldsymbol{r}_1',t)E_N^*(\boldsymbol{r}_2',t)dt &= 0 \quad \text{for } \boldsymbol{r}_1' \neq \boldsymbol{r}_2' \\ &= \frac{1}{\tau}\int_0^\tau \left|E_N(\boldsymbol{r}_1',t)\right|^2 dt\,\frac{\delta^2(\boldsymbol{r}_1'-\boldsymbol{r}_2')}{A} \quad ,\end{aligned} \tag{16.4}$$

where $A = \int da_1' = \int da_2'$ is the area of the object on the celestial sphere. Integration over one or the other of a_1' and a_2' is trivial; we integrate over one and drop the subscript of the other to produce

$$\Gamma(\boldsymbol{\kappa}_1,\boldsymbol{\kappa}_2,0) = \frac{1}{\lambda^2 r^2}\iint \left\langle \left|E_N(\boldsymbol{r}',t)\right|^2 \right\rangle e^{-i(\boldsymbol{\kappa}_1-\boldsymbol{\kappa}_2)\cdot\boldsymbol{r}'}\,da' \quad . \tag{16.5}$$

Note that the integrand now contains the main part of the intensity as a function of position within the object:

$$I_S(\boldsymbol{r}') = \frac{c}{8\pi}\left\langle \left|E_N(\boldsymbol{r}',t)\right|^2 \right\rangle \quad . \tag{16.6}$$

Let us assume furthermore that the far-field measurements are in the *x*-*y* plane, parallel to the $x'-y'$ plane. To first order in the coordinates of the measurement points,

$$\boldsymbol{\kappa} = \frac{2\pi}{\lambda r}\left(x\hat{\boldsymbol{x}} + y\hat{\boldsymbol{y}}\right) + \frac{2\pi}{\lambda}\hat{\boldsymbol{z}} \quad , \tag{16.7}$$

so the wavevector difference that appears in Equation 16.5 is

$$\boldsymbol{\kappa}_1 - \boldsymbol{\kappa}_2 = \frac{2\pi}{\lambda r}\left[(x_1-x_2)\hat{\boldsymbol{x}} + (y_1-y_2)\hat{\boldsymbol{y}}\right] = \frac{2\pi}{r}\left[u\hat{\boldsymbol{x}} + v\hat{\boldsymbol{y}}\right] \quad , \tag{16.8}$$

where we have defined a coordinate system parallel to *x*-*y* but measured in wavelengths: the *u*-*v* plane. Furthermore, in terms of small angles ℓ and m measured by the observers with respect to the origin of the $x'-y'$ coordinate system (see Figure 16.1) we can write

$$\boldsymbol{r}' = r\left(\ell\hat{\boldsymbol{x}} + m\hat{\boldsymbol{y}}\right) \tag{16.9}$$

and

$$da' = dx'dy' = r^2 d\ell dm = r^2 d\Omega \quad . \tag{16.10}$$

Now we can insert Equations 16.6-16.10 into Equation 16.5 to produce

$$\Gamma(u,v,0) = \frac{8\pi}{c\lambda^2} \int_{-\infty}^{\infty} \int_{-\infty}^{\infty} I_S(\ell,m) e^{-2\pi i(u\ell+vm)} d\ell\, dm \quad . \tag{16.11}$$

This is one form of the theorem derived independently by van Cittert in the 1930s and by Zernike * in the 1950s. The result is of major importance: the mutual coherence and the intensity distribution of the object are, apart from the constant factors in front of the integrals, Fourier transforms of one another. The mutual coherence $\Gamma(u,v,0)$ measured at one point in the *u-v* plane gives one Fourier component of the object's intensity distribution. One can therefore generate the *image* of a celestial source by making measurements of the mutual coherence and performing the inverse transform:

$$I_S(\ell,m) = \frac{c\lambda^2}{4(2\pi)^3} \int_{-\infty}^{\infty} \int_{-\infty}^{\infty} \Gamma(u,v,0) e^{2\pi i(u\ell+vm)} du\, dv \quad . \tag{16.12}$$

The point is that the mutual coherence $\Gamma(u,v,0)$ can be measured at points far apart, much farther apart than two points on a realizable telescope, and thus we can achieve much higher angular resolution than with a single telescope.

Measurements of the mutual coherence are composed of two measurements of the far field, with independent radio telescopes and detectors whose signals give the amplitude and phase of the electric field on the telescope primary. These signals are multiplied and integrated electronically, as indicated schematically in Figure 16.1. The departure of the *baseline* vector $\boldsymbol{b} = u\hat{\boldsymbol{x}} + v\hat{\boldsymbol{y}} + w\hat{\boldsymbol{z}}$ connecting the two telescopes (which are mounted, of course, on the Earth's surface) from the *u-v* plane parallel to the celestial sphere needs to be corrected so that the field measurements refer to the same phase of the incoming electromagnetic waves. If the telescopes are pointed along a unit vector $\hat{\boldsymbol{s}}_0$, one telescope's measurements suffers a time delay of

$$\tau_g = -\boldsymbol{b} \cdot \hat{\boldsymbol{s}}_0 \lambda / c \quad , \tag{16.13}$$

with respect to the other, which is corrected by insertion of an appropriate time delay electronically in the signal line of the other telescope, before correlation. The correlator itself is a box of electronics that multiplies together the complex signals – generally voltage waveforms for which the amplitude and phase bear a simple relation to those of the electric field on the telescope primaries – and integrates over time in order to produce a voltage at the output that is proportional to the mutual coherence. One such measurement thus gives, within a proportionality constant that can be calibrated, one Fourier component of the celestial object's intensity distribution.

Arrival at Equation 16.12 is the easy part of spatial interferometry. The performance of suitable measurements of the mutual coherence, and the details of the inverse Fourier transform of the data important in the production of high-fidelity images, involve a great deal more science, and even a substantial amount of art. Measurement of the far field is a topic we will discuss in a couple of weeks, when we introduce the notion of *heterodyne* (or *coherent*) detection.

From its beginnings in the 1950s, interferometry was one of the most important observing techniques in radio astronomy, because it alone offered the chance to achieve angular resolution in radio images that

---

* Frits Zernike also made many other important contributions to physical optics, including the invention of the phase-contrast microscope, for which he won the 1953 Nobel Prize in physics.

Figure 16.2: The NRAO Very Large Array (VLA) in its most compact configuration, called the "D array," viewed from the north.

approached that in visible-light photographs †. It really hit its stride, however, with the commissioning in the early 1980s of the US NRAO Very Large Array (VLA), which can produce radio images with higher resolution and quality than can be obtained at short wavelengths from ground-based visible and infrared telescopes. The VLA, located on the Plains of St. Augustine, between Magdalena and Datil, New Mexico, consists of twenty-seven 25 m diameter radio telescopes. These dishes can be moved among a large number of positions laid out in a Y shape, with the stem of the Y pointing north. In their most widespread configuration ("A array") the largest distance between two telescopes is about 36 km, so in principle the angular resolution at the shortest wavelength of operation (about 7 mm) can approach 0.04 arcseconds. The total collecting area of the telescopes is equal to that of a 130 m diameter telescope, so the VLA can in principle detect fainter sources than any other radio telescope except Arecibo.

The limitation on how far apart the elements of an interferometer can be placed is determined by the accuracy to which one can determine the geometrical delays. With atomic frequency standards the limit is larger than the diameter of the Earth; thus radio astronomers have used interferometers whose elements

---

† Cambridge University radio astronomers Sir Martin Ryle and Antony Hewish received the 1974 Nobel Prize in physics, in recognition of their contributions to the invention and development of radio-astronomical interferometry.

Figure 16.3: the six-element Millimeter Array at Caltech's Owens Valley Radio Observatory. The telescopes are 10.4 m in diameter and have good enough surface quality to operate at wavelengths below 1 mm.

are literally at opposite ends of the Earth to achieve resolution of 10^{-3} arcseconds or better. (As they say at NRAO, with this angular resolution you could read a newspaper in New York from the distance of Los Angeles.) The details of observation, and especially the data reduction, with this mode of operation differ significantly from the case of connected-element arrays like the VLA; thus the use of geographically widespread telescopes has its own name, Very Long Baseline Interferometry (VLBI). Using existing, large single-dish telescopes as the elements, VLBI has been carried out since the mid 1960s. Relatively recently a network of ten dedicated telescopes, stretched across the USA from Puerto Rico to Hawaii, was built by NRAO as the Very Long Baseline Array (VLBA); this array has become the premier instrument for VLBI.

Radio-astronomical interferometry has been pushed to shorter wavelengths as telescope surface accuracy and high-frequency radio receiver performance has improved. Since the early 1980s the University of California and Caltech have operated interferometers, respectively at the Hat Creek and Owens Valley radio observatories, that can work at wavelengths shortward of 1 mm, limited more by atmospheric transparency and stability than by the telescopes and receivers themselves. (The OVRO Millimeter Array is shown in Figure 16.3.) Success with these devices has spawned efforts by the Harvard-Smithsonian Center for Astrophysics to build the new Submillimeter Array (SMA) on Mauna Kea, and by NRAO to propose a "very" large millimeter and submillimeter array, to be located in the Chilean Andes near the Atacama Desert.

